

Cosmological black holes as voids progenitors. I. Simulations.

M. Serpico¹, R. D’Abrusco¹, G. Longo^{1,2,3}, C. Stornaiolo^{1,2}

¹ - Department of Physical Sciences, University Federico II of Napoli, ITALY

² - INFN - Napoli Unit, via Cinthia 6, 80100 ITALY

³ - INAF - Napoli Unit, via Moiariello 16, 80131 Napoli, ITALY

Accepted xxxxxxxx; received xxxxxxxx; in original form 2005 July 12

ABSTRACT

Cosmological black holes (CBH), *i.e.* black holes with masses larger than $10^{14} M_{\odot}$, have been proposed as possible progenitors of galaxy voids (Stornaiolo 2002). The presence of a CBH in the central regions of a void should induce significant gravitational lensing effects and in this paper we discuss such gravitational signatures using simulated data. These signatures may be summarized as follows: i) a blind spot in the projected position of the CBH where no objects can be detected; ii) an excess of faint secondary images; iii) an excess of double images having a characteristic angular separation. All these signatures are shown to be detectable in future deep surveys.

Key words: black holes - gravitational lensing - voids - cosmology

1 INTRODUCTION

Voids are among the largest structures known in the Universe with typical diameters ranging between 20 and 85 Mpc. Among the various models so far proposed for their formation, we may quote the one originally introduced in (Friedmann and Piran 2001), accordingly to which voids form from the evolution of negative primordial perturbations in the density field. More in detail, in this model void formation is the result of two correlated processes. The first one is the comoving expansion of these negative fluctuations. The second arises from the biased galaxy formation picture: galaxies are less likely to form in the underdense regions created by this expansion. Several N-body simulations of this formation mechanism based on the cold dark matter scenario (cf. (Benson et al 2003)) produced results which are consistent with observational data. However, it needs to be stressed that the current observational samples of data (void surveys, morphological classification of void galaxies) (Rojas et al 2005) are too small to allow any conclusive test of this or other models.

Another formation mechanism was proposed by Stornaiolo (Stornaiolo 2002). In this scenario the collapse of extremely large wavelength positive perturbations led to the formation of low density/high mass black holes (Cosmological Black Holes or CBH). Voids are then formed by the comoving expansion of the matter surrounding the collapsed perturbation. This model implies that at the center of voids should still exist a very massive ($M > 10^{14} M_{\odot}$) CBH, which should be detectable through the gravitational lensing effects induced on background galaxies. In this paper we

discuss what these effects are and whether they might be actually observable or not.

This paper is structured as follows. In Section 2 we present the simulations which were performed in order to derive the possible gravitational signatures of the CBH, summarized in Section 3. In Section 4 we discuss whether such effects may or may not be observed in existing or ongoing surveys. In Section 5 we draw some conclusions. In a subsequent paper we shall discuss the weak lensing effects possibly induced by a CBH on a background galaxy distribution.

2 THE SIMULATIONS

In order to evaluate the gravitational lensing effects induced by a CBH located in the center of a void we produced two sets of simulations: one set for a reference unperturbed universe, *i.e.* for a void in an otherwise uniform universe (without the CBH) and a second set obtained from the previous by adding a CBH in the center of the void.

In both cases we assumed, for simplicity, an Einstein-de Sitter cosmological background model, with $\Omega_M = 1$, $H_0 = 100h \text{ Km s}^{-1} \text{ Mpc}^{-1}$ and no cosmological constant. We wish to stress that the only effect of a non zero cosmological constant would be to change the relation $D = D(z, H_0, \Omega_M, \Omega_{\Lambda})$ between the distance D and the redshift z of the background galaxies which is involved in the calculation of the apparent magnitudes and of the angular positions. Using approximate expressions (Kantowski and Thomas 2001) it is easy to see that over a redshift range $[0, 0.4]$ the maximum deviation

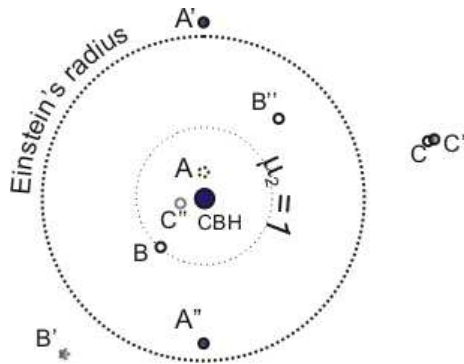


Figure 1. Schematic layout of how the CBH gravitational effects affect the formation of double images as a function of the angular distance of the source from the CBH (see text for a more detailed explanation).

from the standard Einstein-de Sitter model would be of the order of 10%.

As mentioned, the reference universe is described by an Einstein-de Sitter background containing a spherical void of radius R_{void} located at the comoving distance D_{void} from the observer which does not produces any detectable deflection or magnification effects on background galaxies (as pointed out in (Amendola et al 1999)).

The perturbed universe is instead described by a Swiss-Cheese model, with a CBH in the center of the void, which, as above, has comoving radius R_{void} and is located at the comoving distance D_{void} from the observer. The CBH has a mass

$$M = \frac{4}{3} \pi \Omega_{cbh} \rho_{crit} R_{void}^3 \quad (1)$$

where Ω_{cbh} is the density parameter of the CBH. It needs to be stressed that while the background universe is described by a FLRW metric, inside the void region holds a Schwarzschild metric. The boundary conditions at the transition between the two regimes are discussed in (Kantowski 1969). We also assume that changes in the sources redshift, due to the propagation of light across the edge of the void, is negligible. In other words, we describe the void-CBH system as a Schwarzschild lens enclosed in a Einstein-de Sitter cosmological model.

More in particular we simulated a slice of universe covering a solid angle defined by the void diameter and a redshift range comprised between the far edge of the void and $z = 0.4$. This conical volume was populated with a randomly distributed (in the comoving frame) galaxy population drawn from the r -band SDSS (Sloan Digital Sky Survey) luminosity function for the field (Blanton et al 2003). Evolutionary effects induced by the redshift on the luminosity function were neglected. Furthermore we treated galaxies as material points since their physical extension is not relevant to the following discussion.

The lensing effects induced by the CBH were then derived in the weak lensing approximation (Schneider et al 1992) by assuming that the light from the sources passed at a distance from the CBH much larger than its Schwarzschild radius (about 30 arcsec for $M = 10^{14} M_{\odot}$ and $D_{void} = 50 \text{ Mpc}$).

The deflection angle produced by the CBH for radiation approaching with impact parameter ξ is given by

$$\hat{\alpha} = \frac{4GM}{c^2 \xi} \quad (2)$$

For a source at distance D_s from the observer, the Einstein angle can be written in the form:

$$\hat{\alpha}_0 = \sqrt{\frac{4GM}{c^2} \frac{D_{ds}}{D_{void} D_s}} \quad (3)$$

where D_{ds} is the distance of the source from the lens.

If $\hat{\beta}$ is the unlensed angular position of the source with respect to the observer, we know that the effect of the lens will be the creation of two images of the source with angular positions:

$$\hat{\theta}_{1,2} = \frac{1}{2} \left(\hat{\beta} \pm \sqrt{4\hat{\alpha}_0^2 + \hat{\beta}^2} \right) \quad (4)$$

and with magnifications given by:

$$\mu_{1,2} = \frac{1}{4} \left(\frac{\tilde{\beta}}{\sqrt{\tilde{\beta}^2 + 4}} + \frac{\sqrt{\tilde{\beta}^2 + 4}}{\tilde{\beta}} \pm 2 \right) \quad (5)$$

where $\tilde{\beta} = \hat{\beta}/\hat{\alpha}_0$.

Simulations were then performed for different values of Ω_{cbh} and R_{void} (0.05 to 0.4 with step 0.05 and from 10 to 20 Mpc, step 2, respectively).

3 QUALITATIVE DESCRIPTION OF OBSERVABLE QUANTITIES

The simulations showed that the CBH leaves three different types of signatures on the background galaxy distribution. In order to better quantify what happens we refer to Fig. 1 which shows the images produced in three different relative positions of source and lens. When the “real” object (A) is very close to the CBH, we have the formation of two images, namely A' and A'' which are respectively outside and inside the Einstein Radius and very close to it. Both images are brighter than the unlensed image and A' is brighter than A'' . Then when the source moves away from the CBH, the amplification factor with respect to the secondary image tends to 1.

The dashed inner circle marks the position of such locus. If the source B lays on this circle, then it will produce two images B' and B'' . B' is outside of the Einstein Radius at a larger distance than A' and is brighter than B , while B'' lays inside the Einstein Radius closer to the CBH than A'' . Finally let us consider the case of a source C which, if unperturbed would fall outside of the Einstein Radius. Also in this case we shall see two images C' and C'' . The first one will almost coincide with the position of C and will have an almost identical brightness, while C'' will be almost invisible and very close to the CBH.

When a random distribution of background galaxies is considered, the overall effect of the lensing will be the formation of 4 different areas on the sky, namely the regions A , B , C and D , shown in Fig. 2.

The inner circle A , which we call ‘blind spot’, is the region where no image can be detected due to the increasing demagnification of secondary images when they move towards

Ω_{CBH}/R_{void}	10	12	20
0.05	16±5	25±7	36±8
0.2	33±8	36±9	53±10
0.4	39±8	44±9	69±12

Table 1. Average value of θ_{blind} (in arcsec) as a function of Ω_{CBH} and R_{void} (in Mpc). The quoted errors are the r.m.s. of the 1000 individual simulations.

the center of the void. The size of the blind spot depends on the mass of the CBH and on the density of the background galaxy distribution.

The annulus B is characterized by the presence of a large number of secondary images, and it is the second observable feature associated with the CBH.

The third zone C, is an annular zone that we call the 'deficit zone'. It encompasses the average Einstein Radius of the galaxy sample and is characterized by a relatively low number of background galaxy images. It can be understood reminding that, at this angular distance from the center of the void, one can find only those primary and secondary images which originates from sources having angular position falling well within the Einstein Radius. Therefore, in this annulus it is expected to find a lack of both primary and secondary images: as the source moves away from the Einstein Radius, the primary image tends to coincide with the original position of the source while the secondary image becomes fainter and moves more and more towards the CBH.

Finally, the D zone does not present any particular feature produced by lensing, and coincides with the homogeneous background galaxy distribution.

In total we run 48 sets of simulations assuming the void distance at 50 Mpc (*i.e.* matching the distance of the nearest void) and covering a grid defined by: $\Omega_{CBH} = 0.05 \rightarrow 0.4$ with step 0.05, and $R_{void} = 10 \rightarrow 20$ Mpc with step 2 Mpc. For each grid point the procedure was iterated 1000 times randomly changing at each iteration the positions of the background galaxies. Each simulation produced a catalogue of galaxy positions and magnitudes and each group of simulations was then used to derive average quantities.

4 RESULTS

The main observational signatures left by the CBH can be summarized as follows.

4.1 Blind spot

For every simulation, we determined an estimate of the angular radius θ_{blind} of the blind spot, defined as the minimum angular distance from the CBH of the secondary images (brighter than $m_{lim} = 23.5$) and then, at each simulation grid point we took the average value over the 1000 simulations. In Table 1 we list some representative values.

As expected, the size of the blind spot, increases with Ω_{CBH} and with R_{void} . Assuming, for instance, a typical value of 30 arcsec (cf. Table 1), it is apparent that the blind spot should be rather difficult to observe. In fact, while it should be easily detectable in very deep number counts, its

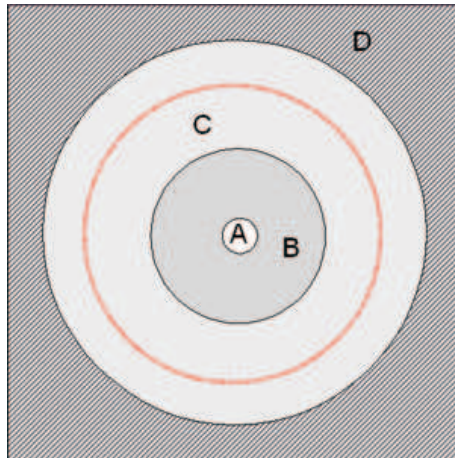


Figure 2. The three regions described in the text. Region A (greatly enlarged to make it visible) is the blind spot; Region B: region where we expect the excess of secondary images; Region C: deficit region (the circle inside the C region shows the average Einstein Radius).

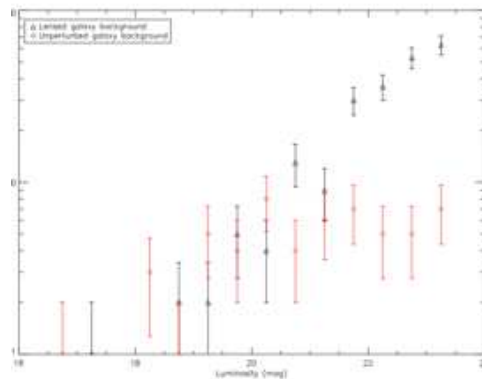


Figure 3. The figure shows in red the average number counts as a function of the apparent magnitude in the r band, obtained, respectively, in the outer region (see text) and in black those obtained in the inner region.

size is of the same order of the average angular separation between bright galaxies at intermediate redshift. Possible effects connected with the distortion induced on extended background objects which happen to fall near the line of sight of the CBH will be addressed in a forthcoming paper.

4.2 Galaxy number counts and radial profile

The presence of the CBH affects the number counts. In order to estimate the size of such effect and in absence of a priori information on the size of the void we adopted the following procedure. First we introduced an annular zone (defining an inner and outer region) centered on the blind spot. The radius of the zone was then found by maximizing the difference between the average galaxy counts in the inner and outer regions.

As it can be seen in Fig. 3, the average number counts associated with the inner area show a systematic difference with respect to those extracted from the background.

This effect however becomes significant only at magnitudes fainter than ~ 21.0 .

In order to quantify such difference we performed a Kolmogorov-Smirnov test on both distributions of points. Each data set was split into two parts including galaxies brighter or fainter than 21 mag, respectively. The brighter parts of the distribution do not present any statistically significant difference, while for the fainter parts we derived a probability higher than 98%, that the two samples are drawn from different populations.

As it was discussed in the previous paragraphs, the presence of a CBH induces a typical pattern in the number counts radial profiles. Such pattern is characterized by a peak in the range of distances intermediate between the blind spot radius and the average Einstein Radius (caused by the secondary images concentration), followed by a dip, which corresponds to a slight underdensity of objects and than at distances comparable with the Einstein Radius it raises up again to smoothly reach the value expected for the background galaxy distribution.

In Fig. 4a we show the number counts profile extracted from the simulation grid-point at $\Omega_{CBH} = 0.2$ and $R_{void} = 12$ Mpc. The first point of the profile is located in the blind spot and is followed by an isolated peak which rapidly falls in the dip.

The only two other examples of possible radial profiles obtained when not placed on the center of the void are illustrated in Fig. 4b and 4c. The first image, which can be roughly described by an initial peak, larger than the previous case, located at the first steps of the profiles followed by the dip, is the typical pattern generated when the central point of the radial profile is positioned inside the secondary images overdensity; the second profile, characterized by the presence of an initial low spot followed by two distinct peaks and the dip, is reproduced when the center of the radial density profile lays out of the circular overdensity created by the secondary images, and inside the deficit annulus.

4.3 Multiple images

The third signature comes just from the pairs of double images produced by the CBH. We expect angular separations for these pairs of the order of two times the average Einstein's angle of the sample. This means angular separations of the order of some arcminutes. This forecast is particularly striking because if these doubles really exist, the only way to observe them practically is to have an estimate of their wide angular separation. We measured the distribution of the angular separation between the double images produced by the CBH obtaining the two points angular correlation function $w(\theta)$ for the simulated galaxy distribution. A standard Landy-Szalay (Landy and Szalay 1993) estimator was used:

$$w(\theta) = \frac{\langle DD \rangle + \langle RR \rangle - 2\langle DR \rangle}{\langle RR \rangle} \quad (6)$$

where $\langle DD \rangle$, $\langle DR \rangle$, $\langle RR \rangle$, are pair counts in bins of $\theta \pm \delta\theta$ of: data-data, data-random and random-random points, respectively. The statistic has been demonstrated to be close to a minimum of variance estimator and to be robust with respect to the number of random points (Kerscher et al 2000).

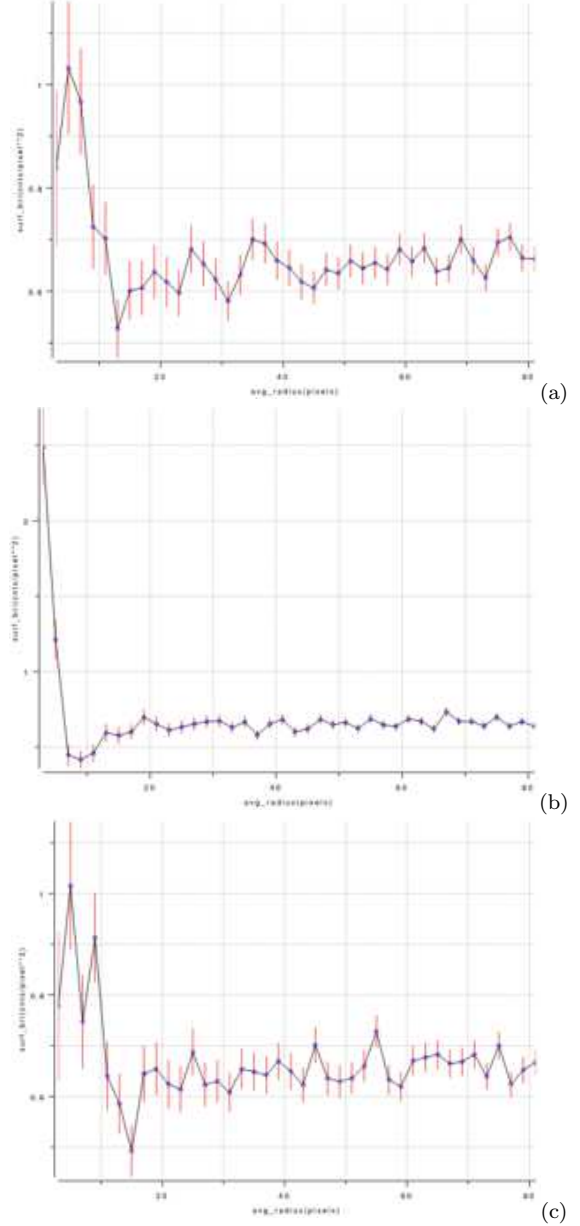


Figure 4. Galaxy number counts radial profiles obtained by integrating over annular regions centered in different regions. Panel a - centered on the blind spot (zone A); Panel b - center falls in the secondary images overdensity region (zone B); Panel c - center falls in the deficit region (zone C).

In Fig. 5 we show the above defined correlation function obtained for the simulation grid-point at $\Omega_{CBH} = 0.2$ and $R_{void} = 12$ Mpc; a well defined peak corresponding to an angular distance of 6 arcmin, comparable with the average diameter of the secondary images overdensity region (Zone B), is visible. Moreover, a slight anticorrelation is found at distance greater than 10 arcmin, while for a random distribution of points no correlation of any sort should be detected. It needs to be stressed that the peak observed at very short angular separations is an artifact produced by the fact that in our simulations galaxies are assumed to be point-like and would disappear if galaxies were approximated with extended objects.

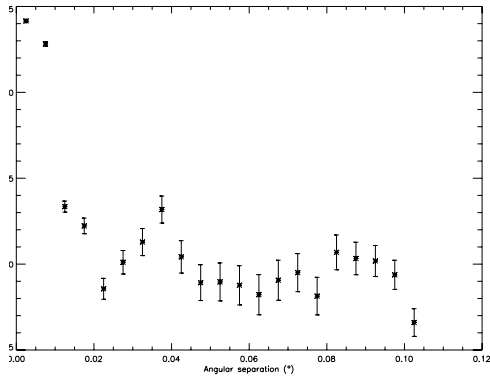


Figure 5. The angular 2-point correlation function derived from the simulated galaxy distribution (see text).

5 DISCUSSION AND CONCLUSION

The results of our simulations which were based on a minimal set of assumptions and can therefore be regarded as quite general and robust in their final predictions, clearly show that the presence of a CBH close to the center of a void would leave unmistakable signatures on the background galaxy distribution as a result of the gravitational lensing properties of the CBH. Unfortunately, they also show that such signatures can be detected only at faint light levels, *i.e.* at magnitudes fainter than the completeness limit of most existing photometric surveys which include voids in their field. Furthermore, the only survey which, at least in theory, should be deep enough to allow at least the radial profile test above described (namely the Sloan Digital Sky Survey, cf. (Stoughton et al 2002)) does not satisfactorily cover any previously known void. It needs to be stressed however that our results clearly show that such tests will be possible on any of the planned deep digital surveys which will become available in the near future (cf. for instance the VST extragalactic survey).

REFERENCES

- Amendola L., Frieman J.A. & Waga L., 1999, MNRAS, 309, 46
 Benson A.J., Hoyle F., Torres F. & Vogeley M.S., 2003, MNRAS, 340, 160
 Blanton M.R., Hogg D.W., Bahcall N.A., Brinkmann J., et al., 2003, ApJ, 592, 819
 Friedmann Y. & Piran T., 2001, ApJ, 548, 1
 Kantowski R., 1969, ApJ, 155, 89
 Kantowski R. & Thomas R.C., 2001, ApJ, 561, 491
 Kerscher M., Szapudi I., Szalay A.S., 2000, ApJ, 335, L13
 Landy S.D. & Szalay A.S., 1993, ApJ, 412, 64
 Rojas R.R., Vogeley M.S., Hoyle F. & Brinkmann J., 2005, ApJ, 624, 571
 Schneider P., Ehlers J. & Falco E.E. *Gravitational Lenses*, Springer
 Stornaiolo C., 2002, Gen. Rel. & Grav., 34, 2089
 Stoughton C., Lupton R.H., Bernardi M., Blanton M.R., et al., 2002, AJ, 123, 485